Grain-boundary segregation of indium in cobalt monoxide

S. P. HOWLETT, R. J. BROOK
Department of Ceramics, University of Leeds, UK

M. GETTINGS
Materials Development Division, AERE Harwell, UK

The composition of the grain boundaries in hot-pressed polycrystalline samples of CoO containing varying levels of indium as a dopant has been investigated using Auger electron spectroscopy and X-ray photoelectron spectroscopy. Segregation of the indium to the grain boundaries has been observed and both the boundary enrichment level and the depth of the segregated layer have been found to vary as functions of additive concentration, annealing temperature and quenching rate. Models based on the existence of space charges or on strain energy terms are both unsatisfactory for the interpretation of the data obtained; it is believed that a contribution to segregation from non-equilibrium processes occurring during cooling must be present.

1. Introduction

The influence of grain-boundary phenomena on the fabrication and properties of ceramic materials is well recognized [1]; the composition of the grain-boundary region has, in particular, been seen as significant in determining the behaviour of ceramic products. The segregation of additives and impurities to grain boundaries in several oxide systems has been studied by a variety of techniques [2–4]; Jorgensen *et al.* [4] have, for example, studied the segregation of MgO in Al_2O_3 using microhardness measurements: the MgO concentrations and the cooling rates employed in this work suggest, however, that second-phase precipitates may have been present. Later studies of this same system using Auger electron spectroscopy (AES) [5, 6], and X-ray photoelectron spectroscopy (XPS) [7] have been hampered by the poor instrument sensitivity to the host (Al^{3+}) and dopant (Mg^{2+}) cations; furthermore, the high dopant levels and slow cooling rates used during specimen preparation have added to these difficulties. Johnson *et al.* [6] have investigated grain-boundary segregation in MgO by using AES and have clearly detected Ca^{2+} and Fe^{2+} enrichment in a 5 nm region at the grain boundary.

Recently, scanning transmission electron micro-scopy (STEM), has been used to investigate segregation in MgO [8] and in other oxides [9]. STEM has the advantage that direct structural observation of the grain-boundary region can be made before chemical analysis; however, the poor spatial resolution and lack of instrument sensitivity can make it difficult to determine the precise segregation profiles. In contrast, the surface specific techniques such as AES and XPS combine a relatively high sensitivity and an exceptional depth sensitivity (typically 1 to 2 nm). XPS has the additional advantage that information concerning the chemical state of the ionic species that are present may be obtained by studying peak shifts and the fine spectral structure [10].

In the present work, AES and XPS have been used to investigate the influence of various In_2O_3 additions on the grain-boundary chemistry of high-purity polycrystalline CoO. This system has the advantage of good discrimination between the host and dopant cations during compositional analysis by AES and XPS [10].

2. Experimental procedure
2.1. Specimen preparation

Batches of CoO containing different additions of In^{3+} (135 to 5380 ppm cation fraction) were pre-

pared by a slurry doping technique. The starting material used was "Spec Pure" Co_3O_4 (Johnson Matthey Ltd) of 10 ppm total cation impurity. The Co_3O_4 was calcined at $1050°C$ in a low p_{O_2} atmosphere (white spot nitrogen) to produce CoO which was subsequently milled with CoO grinding media in a polyethylene container. Reagent grade indium nitrate (BDH Chemicals) was used for the doping. Various selected amounts of indium nitrate were mixed with CoO in triply distilled, deionized water to form a slurry, which was then evaporated to dryness by infra-red heating from above, and by a hot plate below, while stirring continuously. The nitrate radical was decomposed by calcining the dried slurry at $150°C$.

Polycrystalline CoO samples were prepared by hot-pressing: batches of approximately 20 g doped powder were placed in a 1 in. diameter, Nimonic 115 (Henry Wiggin Co Ltd) die and hot pressed to approximately 99% of the theoretical density using punches of the same alloy. The inner die wall and the ends of the punches were coated with a thin layer of boron nitride to facilitate specimen extraction. Hot-pressings were conducted in air at $1100°C$ using an applied pressure of 105 MPa for 15 min, the compact being extracted while still hot.

Rectangular bar specimens, 25 mm × 5 mm × 5 mm, were machined from the hot-pressed billets for the segregation studies. The specimens were individually heat treated by being suspended in a Pt-wire cage in the hot-zone of a vertical tube furnace. Owing to the chemical instability of CoO when cooled in air [12], a low oxygen pressure (10^{-5} atm) was maintained in the furnace during and after the heat treatment to prevent the formation of Co_3O_4 during cooling. The heat treatments were conducted at $1250°C$ or $1100°C$ for $2\frac{1}{4}$ h or 10 h respectively, followed by rapid quenching at approximately $400°C\,min^{-1}$ to room temperature.

All samples were coated with a thin layer of evaporated gold of approximately 10 nm thickness prior to their examination by the surface analysis technique. The presence of the gold film helped to reduce charging effects during the electron bombardment employed in AES analysis and assisted also in the alignment of the fracture surface with the X-ray beam during XPS analysis where a relatively large beam diameter is used.

2.2. Surface analysis
Surfaces analyses were obtained using a PH1-

Balzers electron spectrometer which has been described in detail elsewhere [13]. Facilities for both AES and XPS analysis were available in one ultra-high vacuum chamber, with the optimum sample positions for both AES and XPS analysis being coincident.

For the AES analyses, a 2 kV electron beam with a spot size of approximately $30\,\mu m$ diameter was used. In the mode for XPS analysis, the specimen was bombarded over an area of approximately 3 mm diameter with $AlK\alpha$ X-radiation of characteristic energy 1486.6 eV.

Several specimens were loaded into the spectrometer simultaneously by means of a multi-specimen carousel; the samples were then fractured in high vacuum using a fracture stage and an impact hammer fitted as part of the analysis chamber. Both fracture and analysis of the specimens were conducted at a vacuum of typically 5×10^{-9} torr. The distribution of the dopant beneath the fracture surface (the depth profile) was studied by bombarding the surface with 2 kV argon ions at normal incidence with a current density of $50\,\mu A\,cm^{-2}$ for various times, chemical analysis being performed after each bombardment.

3. Results
Fig. 1 shows a fracture surface of CoO + 0.2 wt% In_2O_3, the predominantly intergranular mode of fracture being typical of all the samples measured. Figs 2 and 3 present, respectively, a typical AES spectrum of an as-fractured specimen showing clearly the Co, O and In Auger peaks and a wide-scan XPS spectrum with the relevant excitations marked. Both spectra are free from signals caused by impurities segregated to the grain boundaries.

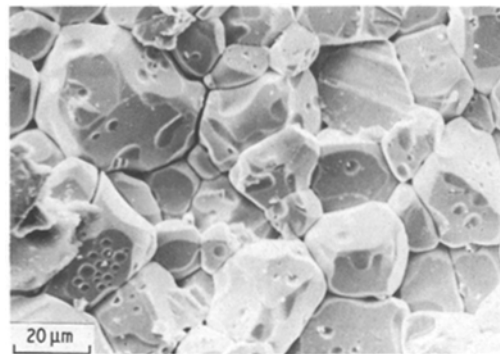Quantitative compositional information is

Figure 1 Fracture surface of CoO + 0.2 wt% In_2O_3 used for surface analysis. Note the predominantly intergranular mode of fracture.
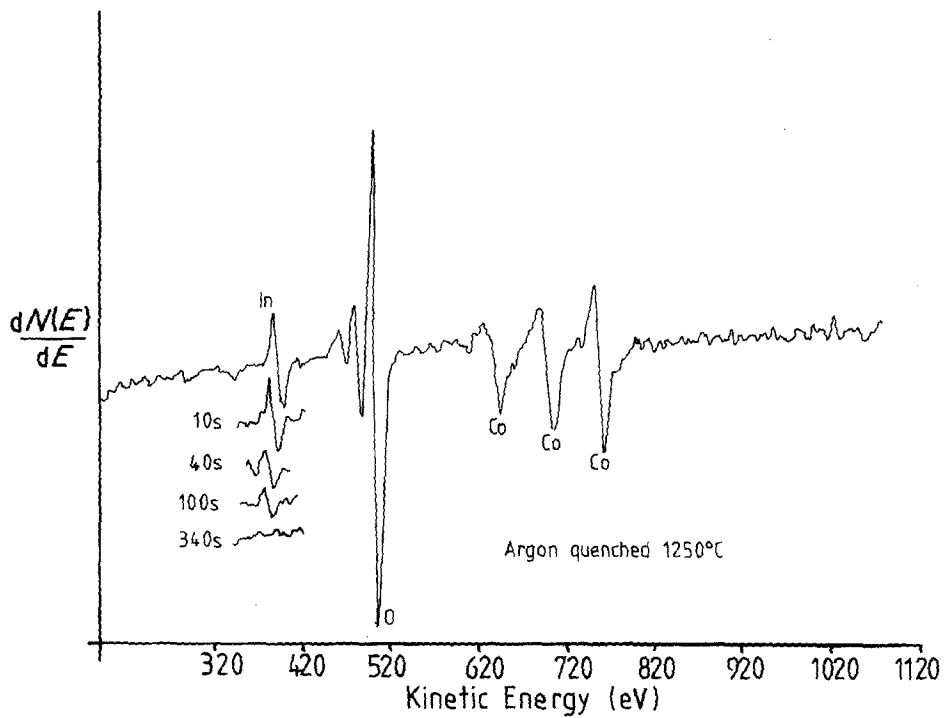
Figure 2 Auger spectra for CoO + 0.1 wt% In_2O_3 showing the effect of argon ion bombardment (sec at $50\,\mu A\,cm^{-2}$ current density) on In peak height.
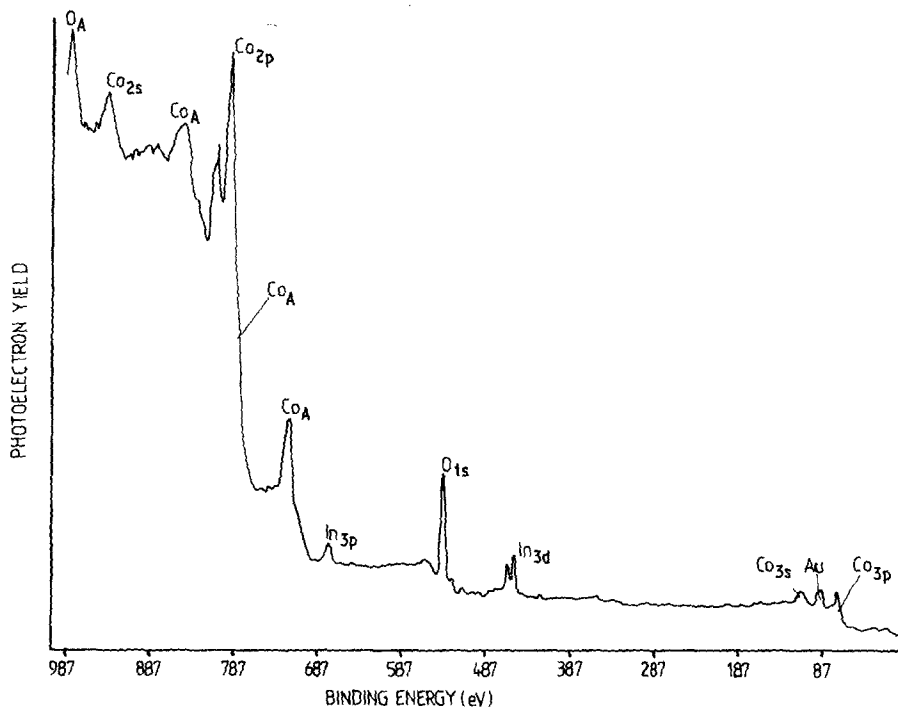

Figure 3 Wide scan XPS spectrum for CoO + 0.2 wt% In_2O_3 (as-fractured).

obtained using the appropriate sensitivity factors and the Auger peak heights and the XPS peak areas. Difficulties in obtaining reliable peak area measurements for the Co_{2p} XPS peak of binding energy 780 eV can be encountered because of the overlapping of this peak with the cobalt Auger peaks at electron energies 775, 716 and 656 eV. Hence, grain-boundary enrichment values have been calculated from the ratio of peak heights of the In and Co Auger peaks.

Detailed photoelectron spectra of the Co_{2p} and O_{1s} transitions have been used in the XPS studies to determine accurately the peak position and shape; this has then provided further information on the chemical state of the cobalt and oxygen ions at the grain boundary. Detailed XPS traces of the O_{1s} and Co_{2p} peaks taken from the as-fractured surface of the sample with composition, $CoO + 0.2$ wt% In_2O_3, are shown in Figs 4 and 5, respectively, together with the spectra taken after an argon ion bombardment of 20 sec duration at a current density of $50 \mu A\, cm^{-2}$. No shift in the relative positions of the O_{1s} and Co_{2p} peaks can be seen between the spectra taken before and after

bombardment. The satellite peaks present in association with the Co_{2p} peaks are characteristic of Co^{2+} ions [14], no such peaks being found if Co^{3+} predominates [14]. Fig. 3 shows the effect of argon ion bombardment (at $50 \mu A\, cm^{-2}$) on the indium Auger peak height as the surface is eroded, i.e. as one moves away from the grain boundary. Segregation profiles of the grain boundary (concentration of dopant as a function of bombardment time) are shown for different dopant concentrations in Fig. 6; it can be seen that an increasing additive concentration enhances both the degree of grain-boundary enrichment and the depth of the enriched region. At a concentration of 2.5 wt% In_2O_3, the profile shape becomes irregular, most probably because the solubility limit of In_2O_3 in CoO has been exceeded. This interpretation is consistent with measurements of the influence of In_2O_3 additions on the kinetics of grain growth in CoO, where the solubility limit has been found to be 0.5 wt% In_2O_3 at 1250° C [15]. The effect of the heat-treatment temperature on grain-boundary enrichment is shown in Fig. 7; a lowering of the annealing temperature reduces
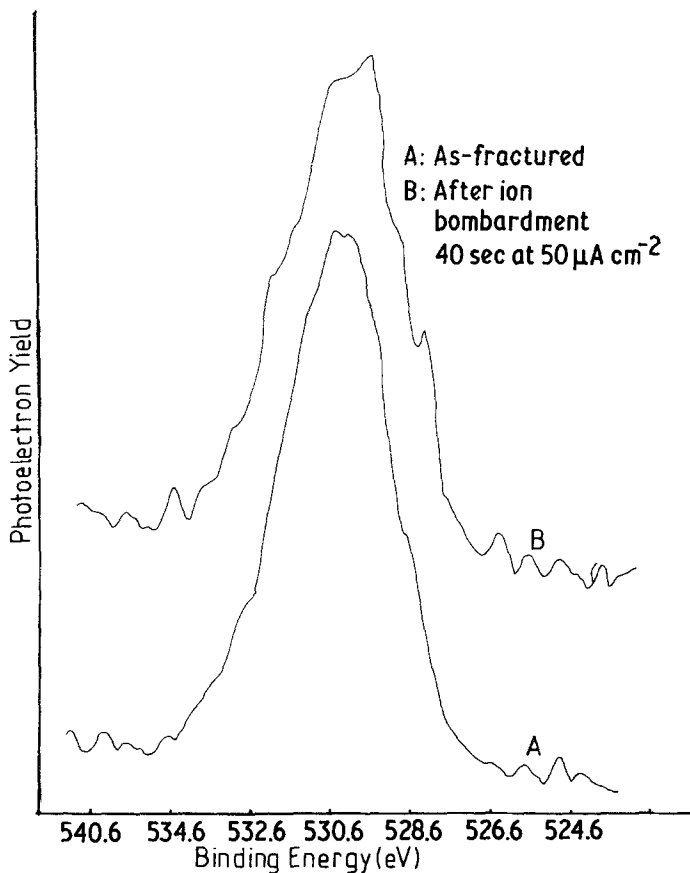
A: As-fractured
B: After ion
   bombardment
   40 sec at 50 μA cm⁻²

Photoelectron Yield

540.6   534.6   532.6   530.6   528.6   526.6   524.6
Binding Energy (eV)

Figure 4 Detailed XPS spectra comparing the O_{1s} photoelectron peaks before and after argon ion bombardment for CoO + 0.05 wt% In_2O_3.
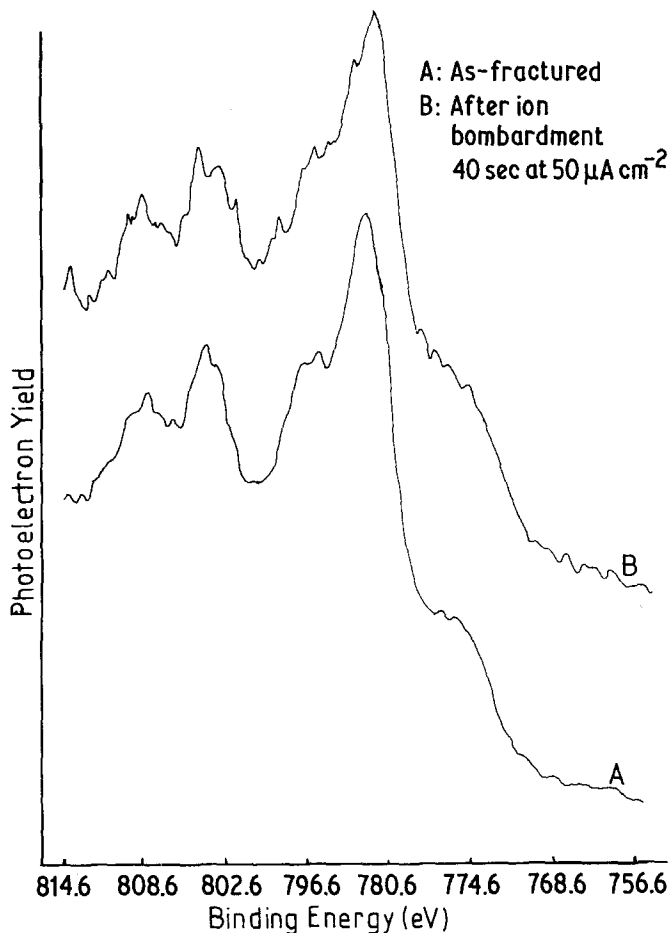
A: As-fractured
B: After ion
bombardment
40 sec at 50 μA cm^{-2}

Figure 5 Detailed XPS spectra comparing the $Co_{2p}{}^{1/2}$ photoelectron peaks before and after argon ion bombardment for $CoO + 0.05\,wt\%\,In_2O_3$.

both the degree of boundary enrichment and the depth of segregation.

The detection limit indicated in Figs 6, 7, 9 and 10 is the concentration at which the In_A peak height became indistinguishable from the background noise level of the spectrum.

4. Discussion

The absence of Co^{3+} from the fracture surfaces during XPS "detailed scan" analyses suggests that Co_3O_4 precipitates are not present as a grain-boundary second phase. The segregation of In^{3+} is therefore occurring within the CoO phase, and is not caused by preferential occurrence of indium in Co_3O_4 precipitates. Fig. 8 shows a typical microstructure of an Ar-quenched sample similar to those prepared for analysis; again no evidence of any precipitates at the grain boundary can be seen.

Equilibrium segregation in ionic solids is commonly interpreted in terms of one or other of two models. First, the surfaces and grain boundaries of an ionic solid in thermodynamic equili-

brium can carry an electric potential resulting from the presence of an excess of ions of one sign [16, 17]; the charge developed at the boundary is linked to the formation of a space charge region of opposite sign adjacent to the boundary which balances the grain-boundary charge exactly. For a pure material, such a space charge is developed when the free energies of formation of the major cationic and anionic point defects differ. The magnitude and sign of the boundary charge (and that of the compensating space charge) vary in the presence of aliovalent solutes owing to interactions between the crystal defect concentrations. The shape of the segregation profile produced by space-charge segregation is that of an approximately exponential decay of the concentration of the segregated species with increasing distance from the grain boundary [18]. Fig. 9 shows the experimental segregation profile tested against the form of the space charge predicted by this model. Only at a dopant level of 135 ppm In^{3+} is an exponential dependence found. Furthermore, as a
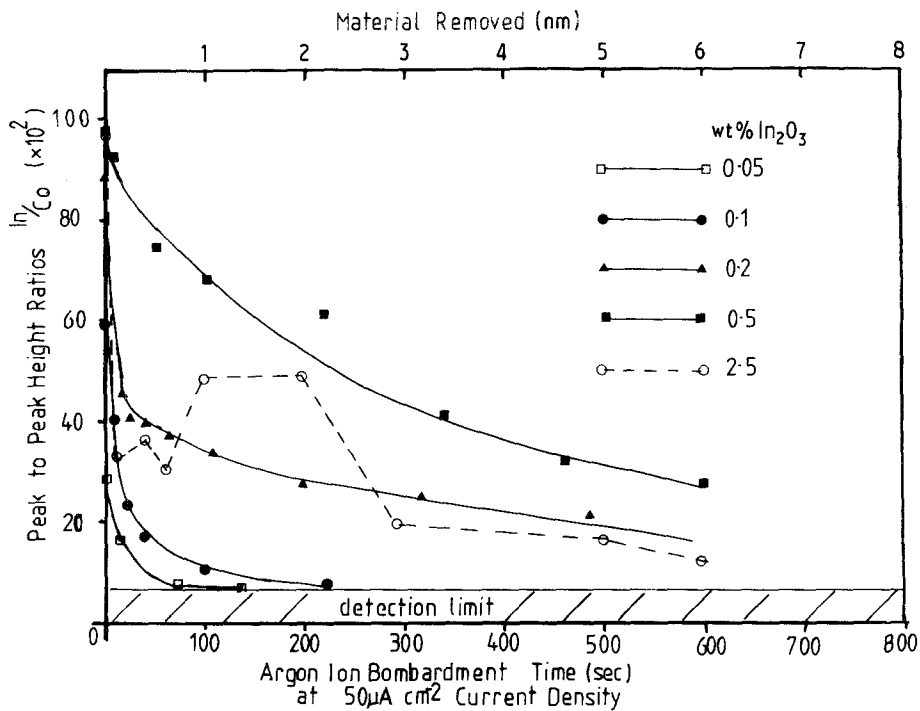
3312

Figure 6 Sputter etch concentration profiles of In_2O_3-doped CoO for various dopant concentrations.

consequence of the space charge model, the Debye length (a measure of the depth of the segregation region) should decrease with increasing dopant level. Table I shows Debye lengths, X_D, calculated from the equation for the case of In^{3+} in cobalt monoxide, namely,

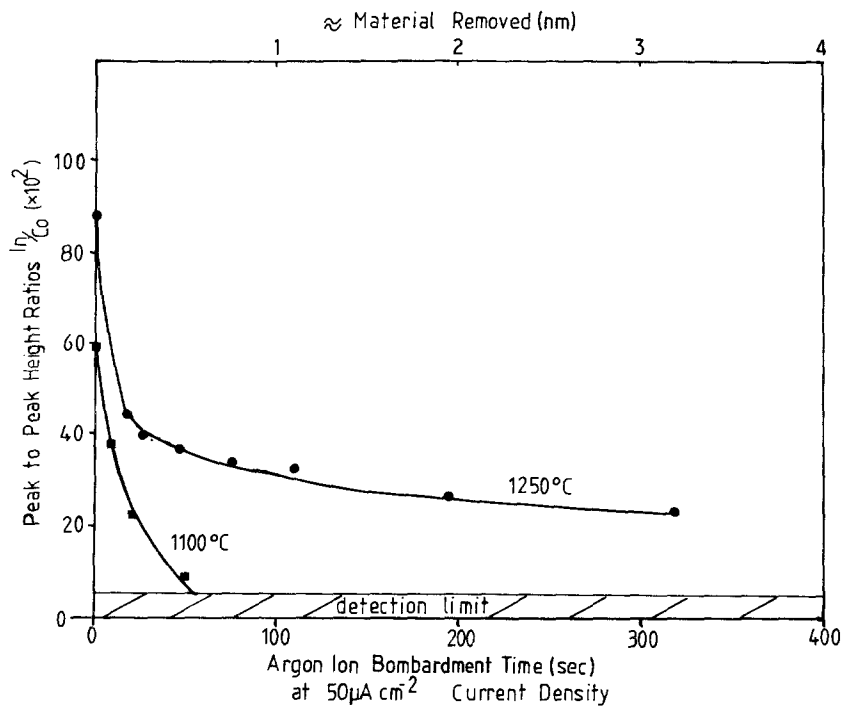$$X_D = \left(\frac{8\pi Nq^2C}{\epsilon kT} \right)^{-1/2},$$

Figure 7 The effect of annealing temperature on the concentration depth profiles for CoO + 0.1 wt% In_2O_3.
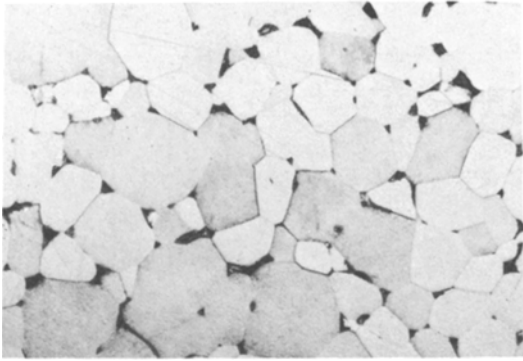
Figure 8 A typical reflected light optical micrograph of an argon-quenched Auger specimen. No second phase can be seen.

where q is the electronic charge (1.6×10^{-19} C), N is Avogadro's number (2.25×10^{28} m^{-3}), ϵ is the dielectric constant (2.25×10^{-10} F m^{-1}) [21], and C the bulk impurity concentration.

At higher dopant levels, 540 and 1350 ppm, the calculated Debye length is particularly small when compared with the observed depth of segregation. At lower dopant levels, a more reasonable agreement between the calculated and observed enrichment depths is found; furthermore, the linear dependence found in Fig. 9 for CoO + 135 ppm In would indicate that electrostatic effects could be responsible for the observed segregation in this material. However, as Table I indicates, increasing dopant levels show the wrong trend in terms of their influence on the enrichment layer thickness and hence the apparent agreement between theory and experiment for the CoO + 135 ppm In^{3+} sample may be fortuitous.

The effects of varying annealing temperature on both the extent of boundary enrichment and the depth of segregation are shown in Fig. 10. These data contradict the predictions of Kliewer and Koehler [17] for space charge-controlled segregation, where any reduction in the annealing temperature should increase the boundary layer thickness and the extent of grain-boundary enrichment observed.
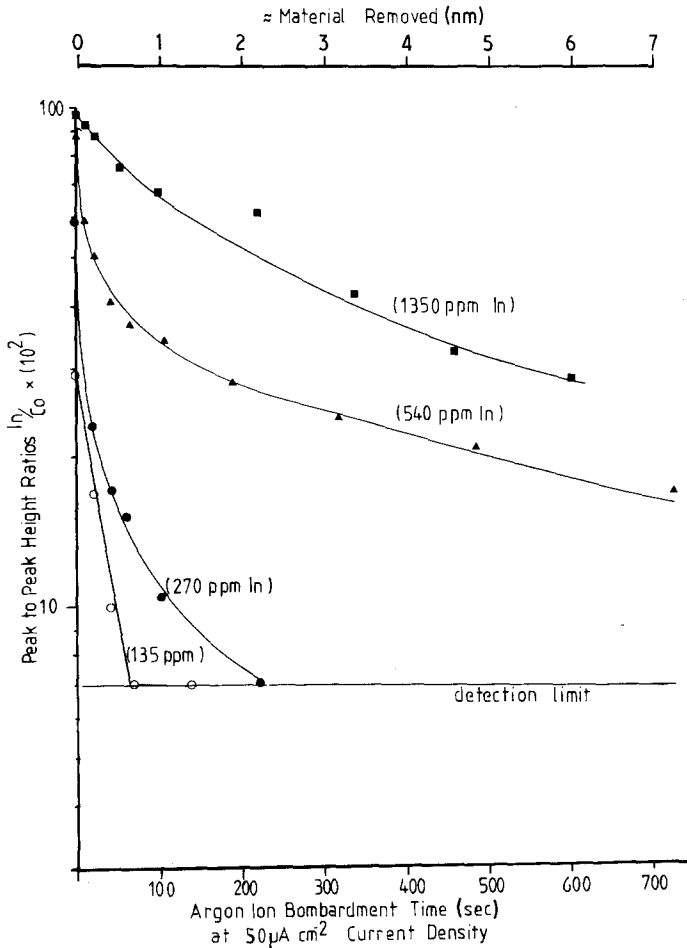

Figure 9 Test of the experimental segregation profile against the ideal shape predicted by the space-charge model.

TABLE I

Debye length, X_D (nm)	Bulk In^{3+} dopant level (ppm)
1.5	135
1.0	270
0.8	540
0.4	1350

From the experimental evidence, therefore, the conclusion is that electrostatic grain-boundary potentials cannot be adequately used to explain the phenomena observed.

The second model for the interpretation of equilibrium segregation is based on strain-energy effects induced by differences between the ionic radii of the host and additive ions. Johnson [19] has used this approach to explain the segregation of various aliovalent solutes in Al_2O_3 and in MgO matrices using a model proposed by McLean [20] for the strain energy induced in a lattice by the introduction of larger solute ions. In CoO doped with In_2O_3, however, the degree of ionic mismatch between the In^{3+} and Co^{2+} ions is small ($\Delta r/r_{host} = 0.07$) compared with $+0.89$ for Ca^{2+} in Al_2O_3 (where pronounced segregation occurs). A more comparable ionic mismatch is found for Si^{4+} in Al_2O_3 where no discernible tendency to segregate to the grain boundaries has been found.

The relatively high levels of grain-boundary enrichment found during this work may not,

therefore, be satisfactorily explained on the basis of such strain-energy arguments.

Since neither model for equilibrium segregation adequately explains the experimental data, it becomes necessary to consider the possibility of *non*-equilibrium segregation induced during cooling. Fig. 10 shows that the cooling rate affects the shape of the segregation profiles and the extent of enrichment produced in CoO + 0.5 wt% In_2O_3. The results indicate that the rapidly cooled samples (quenched at $400°\,C\,min^{-1}$) may still not be cooled sufficiently rapidly for the prevention of segregation during cooling. Mitamura *et al.* [8] have observed differences in segregation as a function of cooling cycle in doped MgO; however, they have employed cooling rates much slower than those used in this work. For the present system, the relatively high cation and anion diffusivities may allow rapid movement of the dopant ions during cooling, preventing any "quenching-in" of the equilibrium segregation profile, and leading to a degree of non-equilibrium segregation. While some data for the lowest dopant level tends to support a space charge segregation model, the bulk of the experimental evidence does not fit this model. Consequently, it is believed that the segregation observed has been dominated by a contribution from non-equilibrium segregation occurring during cooling.

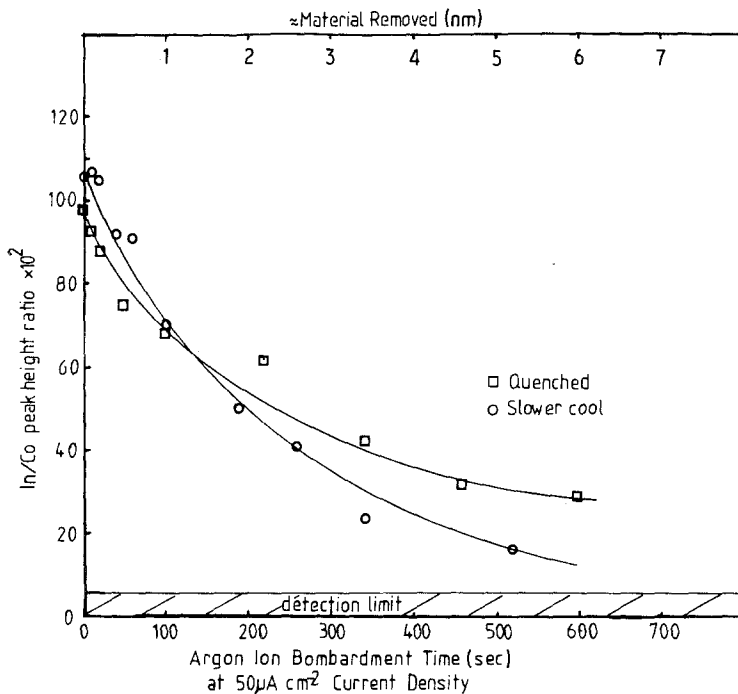To observe true thermodynamic segregation

Figure 10 Segregation profiles for CoO + 0.5 wt% In_2O_3 showing the effect of cooling rate on the profile shape.

without the risk of any interference from cooling effects, grain-boundary analyses must be conducted at the equilibrium temperature; unfortunately, such studies are at present not compatible with the equipment and with the procedures available for grain-boundary study.

5. Conclusions

(1) Solute segregation of In^{3+} to grain boundaries in CoO can readily be detected using AES and XPS techniques on polycrystalline fracture surfaces.

(2) The extent of grain-boundary enrichment and the depths of the segregation layers were found to increase with an increase in the In_2O_3 concentration. At higher concentrations of additive (2.5 wt% In_2O_3), evidence for grain-boundary precipitation was found in the form of the existence of irregular segregation profiles.

(3) Space charge and strain energy models both provide unsatisfactory interpretation of the data obtained; it is believed that a contribution to segregation from non-equilibrium processes occurring during cooling must be present.

Acknowledgement

References

1. W. W. KRIEGEL and H. PALMOUR III (eds.), "The Role of Grain Boundaries and Surfaces in Ceramics", Mat. Sci. Res. III (Plenum, New York, 1966).
2. W. D. KINGERY, *J. Amer. Ceram. Soc.* 57 (1974) 1.
3. J. H. WESTBROOK, in "Ceramic Microstructures", edited by R. M. Fulrath and J. A. Pask (Wiley, New York, 1969) p. 231.
4. P. J. JORGENSEN and J. H. WESTBROOK, *J. Amer. Ceram. Soc.* 47 (1964) 332.
5. H. L. MARCUS and M. E. FINE, *ibid.* 55 (1972) 568.
6. W. L. JOHNSON and D. F. STEIN, *ibid.* 58 (1975) 485.
7. R. I. TAYLOR, J. P. COAD and R. J. BROOK, *ibid.* 57 (1974) 539.
8. T. MITAMURA, E. L. HALL, W. D. KINGERY and J. B. VANDER SANDE, *Ceramurgia Int.* 5 (1979) 131.
9. B. BENDER, D. B. WILLIAMS and M. R. NOTIS, *J. Amer. Ceram. Soc.* 63 (1980) 542.
10. D. BRIGGS (ed), "Handbook of X-ray and U.V. Photoelectron Spectroscopy" (Heyden, London, 1977).
11. P. W. PALMBERG, G. E. RIACH, R. E. WEBER and N. C. MACDONALD, "Handbook of Auger Electron Spectroscopy" (Physical Electronics Industries Inc., Edina, Minnesota, 1972).
12. B. FISHER and D. S. TANNHAUSER, *J. Chem. Phys. Solids* 33 (1972) 801.
13. M. GETTINGS and J. P. COAD, *Surface Sci.* 53 (1975) 636.
14. K. KIROKAWA, F. HONDA and M. OKU, *J. Electron Spect. Rel. Phenom.* 6 (1975) 333.
15. S. P. HOWLETT, Ph.D. Thesis, University of Leeds (1981).
16. K. LEHOVEC, *J. Chem. Phys.* 21 (1953) 1123.
17. K. L. KLIEWER and J. S. KOEHLER, *Phys. Rev.* 140 (1965) 1126.
18. F. A. KRÖGER, "The Chemistry of Imperfect Crystals" (North-Holland, Amsterdam, 1965) p. 777.
19. W. C. JOHNSON, *M.E. Trans. A* 8A (1977) 1413.
20. D. McLEAN, "Grain Boundaries in Metals" (Clarendon Press, Oxford, 1957).
21. H. B. LAL and K. G. SRIVASTAVA, *Ind. J. Pure Appl. Phys.* 7 (1969) 70.